Polymer Biocomposites and Nanobiocomposites Obtained from Mango Seeds

Edna M. S. Cordeiro,[1] *Yana L. Nunes*,[1] *Adriano L. A. Mattos*,[1,2] *Morsyleide F. Rosa*,[2] *Men de sá M. Sousa Filho*,[2] *Edson N. Ito**[3]

Summary: The objective of this work is to obtain thermoplastic starch, polymer biocomposites and nanobiocomposites using agro-industrial waste generated in mango processing, and characterize the obtained materials. The starch extraction from the kernels of mango pits showed a good yield and the obtained starch had high purity.The results obtained characterizing the fibers and cellulose nanowhiskers, from the husk of the mango seed, proved the effectiveness of chemical treatment removing the amorphous constituents (hemicellulose and lignin).The polymer biocomposites and nanobiocomposites were obtained and the TPS mango starch showed satisfactory results of mechanical and thermal properties, when compared with TPS corn starch materials with the same composition. It is concluded that the waste generated in the agro-industrial processing of mangos showed a potential source for biodegradable materials production.

Keywords: biopolymers; cellulose nanowhiskers; mango waste, thermoplastic starch

Introduction

The use of synthetic polymers in Brazil is growing. According to the Brazilian Association of the Plastics Industry, in 2011 the consumption reached a significant quantity of 6.89 million tons.[1] The post-consumer and post-industrial polymeric wastes represent a major challenge for waste management in big cities.[2] One way to minimize this problem is the development of new biodegradable materials, reducing or replacing the use of synthetic ones.

The biopolymers global production capacity in 2007 was estimated at 360,000 tons, of which 43% was plasticized starch.[3] However, the use of starch obtained from traditional sources, such as corn, cassava, wheat, rice, and potatoes, can generate undesirable pressure on the prices of these food crops.

The U.S. ethanol production from corn could lead to a 37% increase in the price of this commodity, depending on the scenario considered.[4] Thus, the development of alternative technological routes that allow the use of non-food starch sources is also a very important strategy, in order to prevent undesirable pressure on food commodity prices.

The mango is one of the main fruits of the global agribusiness. In 2010, Brazil produced about 1.18 million tons,[5] and it is estimated that approximately 5 to 6% of the production is absorbed by agribusiness.[6]

The mango seed represents about 13% of the total fruit weight,[7] this percentage is about 50% of endocarp, 2% is the integument, and 48% is kernel.[8]

The estimated mango kernel production was about 4000 tons in 2010 Brazilian crop. Moreover, considering that, these kernels contain approximately 40 to 50% of starch,[8] it is perceived as a potential raw material source for the production of biodegradable polymers.

[1] Programa de Pós-graduação em Ciência e Engenharia de Materiais, Universidade Federal do Rio Grande do Norte, Natal-RN, Brazil
[2] Embrapa Agroindústria Tropical, Fortaleza-CE, Brazil
[3] Departamento de Engenharia de Materiais, Universidade Federal do Rio Grande do Norte, Avenida Senador Salgado Filho, 3000, CEP: 59078-970, Natal-RN, Brazil
E-mail: ito@ufrnet.br

The starch may be gelatinized and transformed into a thermoplastic starch (TPS) by mixing in suitable equipment in the presence of a plasticizer under pressure and temperature.[9] TPS plasticized just by water becomes very brittle at room temperature so we can use other plasticizers such as glycerol, propylene glycol, and sorbitol to increase the flexibility of the material and improve its processing and applicability.

FORSSELL, MIKKILÄ, et al., found that increasing the concentration of plasticizer during the processing of TPS inhibits or retards the crystallization of the amylopectin, lowering the glass transition temperature (Tg). Thus, increasing the concentration of the glycerol plasticizer agent may change the mechanical behavior of the TPS to fragile from rubbery behavior at room temperature.[10]

The performance of the thermoplastic starch (TPS) is limited by low mechanical properties and high water absorption when compared to most commonly used polymers. Therefore, alternative methods have been employed in order to improve its mechanical strength and barrier properties, combining the use of microfibers or cellulose nanowhiskers in matrices of TPS.[11]

Curvelo, Carvalho, and Agnelli evaluated the properties of the TPS composites prepared with corn starch plasticized with 30 wt% glycerin and reinforced with short cellulosic fibers of 16 wt% from bleached pulp of the Eucalyptus urograndis. The TPS composites were prepared in an internal mixer. The mixture was hot pressed in 2–3 mm-thick plates and then cut to prepare the specimens for mechanical tests. The composite shows an increase of 100% in tensile strength, and more than 50% in modulus with respect to non-reinforced thermoplastic starch. The results showed the advantages in the use of thermoplastic starch reinforced with cellulosic fibers; a natural, cheap, and abundant material.[12]

Ma et al., studied the characteristics of corn TPS composites, firstly prepared with urea (20 wt% of starch) and formamide (10 wt% of starch), using micro winceyette fibers as reinforcement (fiber length of about 12mm), and processed in a single screw extruder. The increase of fiber content went from 0 to 20 wt%, with an increase of around 252% in tensile strength and Young's modulus, while the elongation was reduced by about 82%. The reinforcement effect was gradually weakened with the increase of water content, (>30%) while both the fiber and water content had no effect on the tensile strength. This behavior is produced because water can form hydrogen bonds between the starch and fiber, modifying the original interaction.[13]

Corradini et al., studied biodegradable matrix composites using starch/gluten/glycerol in a 40/40/20 wt% proportion and water in the ratio of 10 wt% comparing to a matrix reinforced with 5 to 30 wt% of fibers of sisal. The composites were produced by mixing in an internal mixer connected to a torque rheometer, and the samples were compression molded and than characterized by water absorption and mechanical testing. In the tensile test, the increase in the Young's modulus and ultimate tensile strength were approximately 560% and 162% respectively, and the elongation at break decreased, comparing to the matrix. The addition of sisal fibers in the matrix decreased the water absorption at equilibrium.[14]

Prachayawarakorn, Ruttanabus, and Boonsom prepared thermoplastic rice starch (TPRS) plasticized by glycerol. In order to improve tensile properties and reduce water absorption of the TPRS, cotton fiber or low density polyethylene (LDPE) were added into the TPRS matrix. The results showed that the incorporation of either cotton fiber or LDPE into the TPRS matrix caused the considerable improvement of tensile strength and Young's modulus. Moreover, water absorption of the TPRS samples was clearly reduced by the addition of cotton fiber or LDPE.[15]

Teixeira et al., studied the corn TPS with 30 wt% glycerol, evaluating the effects of adding cotton cellulose nanofibers at concentration of 0.5 to 5.0 wt%. Polymer nanocomposites were processed in a co-rotating twin screw extruder and films were

obtained by hot-pressing process. All compositions had better tensile strength compared to pure TPS. For samples containing 5 wt% nanowhiskers, the Young's modulus, tensile strength, and elongation at break increased 48.5, 150, and 122 wt%, respectively, compared to pure TPS.[16]

Campos et al., obtained polymer bionanocomposite from a mixture of corn starch and glycerol (70/30 wt%), stearic acid (2 wt%), and sisal cellulose nanowhiskers (5 or 10 wt%) processed in twin screw extruder and pelletized. The dry pellets were mixed at 80/20 wt% of the polycaprolactone (PCL) in a twin screw extruder and molded in a single screw extruder to obtain ribbons. Samples containing 5 wt% cellulose nanowhiskers showed an increase of 10% on the Young's modulus, 16% at tensile strenght, and a 44% reduction in elongation at break compared to TPS. The addition of 5 wt% cellulose nanowhiskers in TPS/PCL blend resulted in a 74% increase in Young's modulus, 80% tensile strenght, and a 40% decrease in elongation at break.[17]

Hietala, Mathew and Oksman obtained films of the potato TPS, plasticized with sorbitol (30 wt%), and reinforced with cellulose nanofibers from wood (5–20 wt%). It was found that adding 10 wt% of nanofibers increased the tensile strength 86%, and adding 20 wt% of the nanofibers increased the Young's modulus to 190% compared to pure TPS. The elongation at break was reduced with the addition of cellulose nanofibers.[18]

Thus, this work aims the recovery of the waste from mango processing, the development of biodegradable materials using starch, microfiber and cellulose nanowhiskers extracted from the mango seeds, and the physicochemical, mechanical and morphological characterization of materials obtained.

Experimental Part

Starch Extraction

The Tommy Atkins mangoes were purchased in the local market in Fortaleza, Ceará, Brazil. The starch was isolated from kernels of the mango following the procedure described by Singh, Sandhu, Kaur *et al.*,[19] with modifications. Initially, the kernels were removed from pits, cut into 2–5 cm pieces and placed in plastic beckers containing a solution of sodium metabisulphite 0.5% (w/v) at a ratio of 1:2 (kernels: solution) for 16 h. Then, the solution was drained and the kernels were ground in a semi-industrial blender with distilled water for 5 min. The material obtained was passed through sieves of 60 mesh and 100 mesh respectively, to separate the soluble material from the bagasse. Bagasse retained in the sieves was washed extensively with distilled water to remove as much starch as possible. The filtrate stood for 1 h to settle the starch. The supernatant was removed, and then added the decanted solution of NaOH 0.2% (w/v) in a 1:2 ratio (material: solution) under magnetic stirring for 2 h. The resulting mixture was adjusted to pH 6.0 with HCl 0.5% (v/v) and then centrifuged at a rotation of 13,000 rpm at 4 °C for 15 min (Hitachi High-Speed Refrigerated Centrifuge, CR22GIII), to separate the precipitate clear fraction (rich in starch). Aiming to remove impurities, starch was repeatedly suspended in distilled water and centrifuged until it reached a pH of 7. 70% alcohol was added to the starch stirring. The mixture was allowed to stand. The starch was decanted, and washed with distilled water by vacuum filtration. Finally, the starch obtained was kept in an oven at 40 °C for 24 hours, powdered in mortar and pestle and stored in glass jars.

Kimimo® corn starch was used as the conventional source of starch. Commercial corn starch was washed in advance with distilled water to remove contaminants and then dried at 50 °C for 24 h.

Extraction of Fibers and Cellulose Nanowhiskers

The fibers were extracted from the mango endocarp. Initially, the endocarps were triturated in a Wiley mill blade (Fortinox Star, FT80) using 30 mesh sieve. Treatment with an alkaline solution of 2% NaOH (w/v)

was performed at a 1:20 ratio (fiber: solution) at 80 °C for 2h. Then, the fibers were washed with distilled water by vacuum filtration until pH 7, dried at 50 °C for 24 hours, ground in an analytical mill (IKA, Allbasic) to disintegrate the agglomerates of fibers formed after the drying process.

Then, bleaching was then used to remove the remaining lignin and hemicelluloses. The chosen method for bleaching with hydrogen peroxide leads to less environmental impact than others which use chloride reagents.

The fibers were bleached at a proportion of 1:20 (fiber: solution) with a solution composed of 30% H_2O_2 (v/v) and NaOH 4% (w/v) for 2 h at 50 °C. After treatment, the fibers obtained were washed to attain a neutral pH and dried as mentioned in the alkaline treatment process. The bleached fibers were subjected to acid hydrolysis with sulfuric acid 52% (w/w) in a 1:20 ratio (fiber: solution) under vigorous stirring at 45 °C for 2 h according to the methodology described by Orts *et al.*,[20] with modifications. After hydrolysis, the reaction was terminated with ice-cold deionized water at a ratio of 1:5. The sample was subjected to ultrasound (Unique) for 2 min at power of 99 W, and then centrifuged at a rotation of 13,000 rpm at 4 °C for 15 min. The precipitate was washed with deionized water, underwent ultrasound and then centrifuged under the same conditions. This suspension of cellulose nanowhiskers was dialyzed in ion exchange membrane (regenerated cellulose membrane Biotech, Spectra brand) in water under constant flow until it reached a pH of 7.0, and then dried in lyophilizer (Liotop, L- 202).

Processing

Corn starch was used as reference for the analysis of mango starch, thus all treatments were performed for both the thermoplastic starches (TPS).

Initially, starch (62.5 wt%), glycerol (28.1 wt%), and water (9.4 wt%) were premixed in a mechanical mixer at 5,000 rpm for 10 min. This mixture was kept in polyethylene bags at 4 °C for 24 hours before processing for improved plasticizer absorption. Mixtures of mango starch and corn starch were processed in a co-rotating twin-screw extruder (AX Plastics, AX-DR, D = 16 mm, L/D = 40) with nine heating zones whose temperatures were set at 70/80/105/110/110/100/100/110/120 °C from feed to die at a speed of 180 rpm.

In the next step, TPS composites and nanocomposites were processed into single screw extruder (AX Plastics, D = 16 mm and L/D = 26) with three heating zones whose temperatures were set at 100/110/100 °C from feed to die at a speed of 40 rpm and using a rectangular die to obtain ribbons. Nanowhiskers and cellulose fibers were mixed with TPS before processing. Six samples were obtained: thermoplastic mango starch (MS), thermoplastic corn starch (CS), TPS mango starch nanocomposite with 1 wt% of cellulose nanowhiskers (MS1CN), TPS corn nanocomposite with 1 wt% of cellulose nanowhiskers (CS1CN), TPS mango starch composite 6 wt% of bleached fibers (MS6BF), and TPS corn composite with 6 wt% of bleached fibers (CS6BF).

Raw Material Composition

The kernels of mango fruits and the starch extracted from these were analyzed for moisture content, ash, lipids, proteins, and total starch following methods described in the Standards of the Adolfo Lutz Institute.[21] The amylose content was assayed by colorimetric method as described in standard ISO 6647.[22]

The fibers were chemically characterized as moisture, ash, extractives, lignin and insoluble alfacelulose as described by TAPPI Standards.[23–27] The holocellulose was determined according to the methodology described by Wise and colleagues.[28] The determination of hemicellulose was held by the difference between holocellulose and alfacelulose.

Fourier Transform Infrared Spectroscopy

The samples of untreated fibers, bleached cellulose fibers, and nanowhiskers were analyzed in a Fourier Transform infrared spectrometer (FTIR), brand ABB-Bomem

Model FTLA, in the region 4000–400 cm^{-1}. Samples of cellulose fibers and nanowhiskers of dry KBr were mixed at a ratio of 1:100 (w/w) and tablets prepared. 20 scans were performed on each sample.

X-Ray Diffraction

X-ray diffraction (XRD) patterns of the starch samples, cellulose fibers, and nanowhiskers were recorded in reflection mode in the ranges of 5–40° angles (2θ) at room temperature using a Rigaku diffractometer DMAXB operated in Cu K (λ = 1.5406 Å), scan rate of 1° (2θ). min^{-1} and a step interval of 0.05° (2θ). The radiation from the anode operated at 40 kV, 40 mA. Equation (1) was used to calculate the crystallinity index (I_{CR}) of the samples of fibers:

$$I_{CR} = \left(\frac{|I_{200} - I_{AM}}{I_{200}}\right) \times 100 \quad (1)$$

Where: I_{200} corresponds to maximum intensity of crystal plane (200) at 2θ = 22.5°; and I_{AM} corresponds to lower height between 200 and 110 peaks at 2θ ≈ 17° and 18°, which represents the amorphous material.

Thermogravimetry

Thermogravimetric analysis (TGA) of mango starch was performed on a Mettler Toledo (TGA/SDTA 851), under a nitrogen atmosphere. The samples were heated at 25–800 °C at a heating rate of 20 °C.min^{-1} and a flow rate of nitrogen gas of 50 ml.min^{-1}.

Thermogravimetric analyzes of pulp fibers and nanowhiskers were performed on a Perkin Elmer (STA 6000), under an atmosphere of nitrogen. The samples were heated at 25–700 °C at a heating rate of 10 °C.min^{-1} and a flow rate of nitrogen gas of 30 ml.min^{-1}.

Differential Scanning Calorimetry

Differential scanning calorimetry (DSC) analysis was performed on DSC equipment (TA Instruments Q20), the ratio of heating and cooling was 10 °C.min^{-1} in a nitrogen atmosphere at a rate of 50 mL.min^{-1}. A first heating cycle from −80 °C to 180 °C was conducted and a 1 min isotherm was performed. Then the sample was cooled to −80 °C for a 1 min isotherm. Soon after, a second heating cycle was carried out to 180 °C.

Transmission Electron Microscopy

The morphology of cellulose nanowhiskers was analyzed in a transmission electron microscope (TEM) Tecnai F20 TMG2 (FEI Company, Hillsboro, OR). Aqueous suspensions of cellulose nanowhiskers were sonicated for 30 min, then one drop of the suspension was added on a copper grid of 300 mesh coated with Formvar film. Uranyl acetate was used in 20 wt% for contrast. After 24 h drying, the material was analyzed. Measurements of length and diameter of 100 cellulose nanowhiskers were performed using GIMP 2.6 software.

Scanning Electron Microscopy

The starch and fibers samples were analyzed by scanning electron microscopy (SEM) on a HITACHI equipment TM 3000 model, with magnification 15 to 30.000x operating at accelerating voltage of 5 to 15 kV with a tungsten filament. The starch samples were diluted in PA ethyl alcohol with a proportion of 1:10 (starch: alcohol) and 1 drop of this suspension was placed on tape and fixed to the sample holder, and the SEM analysis was conducted after 24 hours. The fibers samples were drying in a vacuum oven at 50 °C for 24 h and after added to an aluminum sample holder and analyzed. TPS samples, composites, and nanocomposites were fractured in liquid nitrogen. The samples were coated with a thin layer of platinum, using a Emitech model K550, then analyzed in a scanning electron microscope (Philips XL - 30) with an accelerating voltage between 5 and 20 kV.

Mechanical Testing

The samples were produced in ribbon form using a single screw extruder and then was cut using laser to produce specimens in the tie form (ASTM D638-01 type V). The

tensile tests were carried out using an EMIC model DL-3000 equipment. Crosshead displacement rate were of 1 mm.min^{-1} and cell load of 30 kN.

Permeability to Water Vapor

The permeability to water vapor (P_{WV}) was determined gravimetrically according to ASTM E96-00 (ASTM 2000). Permeation cells with 49 mm diameter and 13.2 mm in height containing 6 ml water were used, maintaining a space on the cell height of 10 mm. The disk-shaped films were sealed on top of the cells, which were then placed in a ARSEC-CVD 040 vertical desiccator - circulating air containing silica gel at 0% RH (relative humidity), previously dried at 105 °C for 24 h. Cells were maintained at 25 °C and 30% RH for at least 24h and weighed 8 times over 1 day at intervals of at least 1h. The weight gain was plotted as a function of time. P_{WV} (in g.mm.kPa^{-1}.h^{-1}.m^{-2}) was defined according to equation 2:

$$P_{WV} = \frac{TP_{WV} \times e}{\Delta P} \quad (2)$$

Where the rate TP_{WV} is water vapor permeability (slope of the line divided by the film area), or transmission rate of water vapor (g·m^{-2}·h^{-1}) through the film calculated from the slope of the straight line divided by the exposed area of the film (m^2), the thickness, and ΔP is the difference in partial pressure of water vapor between the faces of the film.

Results and Discussion

Raw Material Composition

The starch extraction from the Tommy Atkins mango kernels showed a yield of 32%, considering the initial mass of kernels (with 39.43% humidity) and the mass of starch extracted from them. Table 1 shows the chemical composition of the mango kernels and starch after drying in an oven.

The starch ash content observed is substantially higher than the observed for kernels, probably due to the presence of sodium cations derived from alkaline treatment and not completely removed in the washing process of the material. Similarly, Mendes[29] found greater ash content (0.4%) for the mango starch.

Table 1.
Chemical characterization of kernels and starch extracted.

Parameters (wt%)	Materials	
	Kernels	Mango Starch
Humidity	10.66	10.74
Ashes	0.01	0.07
Lipids	11.64	0.05
Proteins	4.80	1.14
Total starch	56.70	72.70

Lipids represent an important fraction associated to starch granule, being responsible for setting color, flavor development, and complexing.[30] The presence of lipids in starch films also improves the barrier characteristics to water vapor. The lipid content found for starch (0.05%) is about 232% lower than the lipid content originally found in the kernels of mango pits (11.64%). Medina *et al.*[31] found a lipid content of 2.52% for starch obtained from the kernels of the mango pits. The lipid content can be considered low when presented below 1%.[32]

The protein content was found to be 4.8% for the kernels and 1.14% for the starch. The reduction of protein content is important because during processing, the occurrence of Maillard reactions can lead to yellowing of the material, as reported by Lopez *et al.*[33]

The total starch content was 56.7% and 72.7% of kernels and mango starch, respectively. The purity of the starch found in this study was lower than the figure recorded by Solis,[34] at 96.6%. However, it approaches the required value of starch (minimum of 80% m/m) by Brazilian Legislation.[35]

The amylose content of the starch extracted from the mango kernels was 27%. Similar values were found by Agustiano - Osornio *et al.*,[36] and Solis,[34] who obtained an amylose content of 28.7% and 31.1%, respectively. The amylose content in starch

Table 2.
Chemical Characterization of untreated fibers, and bleached fibers.

Parameters	Untreated Fibers	Bleached Fibers
Moisture	8.81 ± 0.03	8.02 ± 0.03
Ash	0.88 ± 0.04	1.31 ± 0.005
Insoluble lignin	21.07 ± 0.61	7.6 ± 0.40
Hemicellulose	28.63 ± 0.54	8.78 ± 0.65
Alfacellulose	41.47 ± 1.20	63.84 ± 0.09

extracted from the mango kernels is similar to the content shown for corn starch (28%).[37]

Plant fibers have as major components cellulose, hemicellulose and lignin.[38] For its application as reinforcement in polymer composites, it is desirable to remove amorphous constituents (hemicellulose and lignin) and increase the content of alfacellulose, which is the crystalline phase of the fiber. Table 2 shows the mean values of chemical parameters obtained with the respective standard deviation.

It was observed that there was an increase in the treated fibers ash content, probably due to the addition of sodium cations in the bleaching process. The extractive contents were reduced after chemical treatments, indicating the removal of compounds such as volatile oils, terpenes, fatty acids, mono and polysaccharides, alkaloids, and aromatic compounds. The chemical processes have been effective in reducing the lignin and hemicellulose, increasing the relative content of alfacellulose in the chemically treated fibers.

Fourier Transform Infrared Spectroscopy

The spectra in the Fourier transform infrared spectroscopy (FTIR) were used to confirm the chemical composition of lignocellulosic materials based on the identification of organic functional groups. A reduction in the number of peaks can be observed in the spectra of bleached fibers and cellulose nanowhiskers (Figure 1) (highlighted by a dashed line in the figure). This suggests that the chemical treatments reduced the content of hemicellulose and lignin, and confirms the results of the chemical characterization.

The absorption bands in the range of 1000–1200 cm^{-1} are attributed to the stretching of C—OH and C—O bonds present in the lignin and cellulose.[39]

The absorption bands in the range between 1125 and 1000 cm^{-1} attributed to the stretching of C—O, C—C and C—OH hemicellulose bonds,[40] and were observed in all samples.

The absorption in the region 1500 and 1580 cm^{-1} observed in untreated fibers is related to the stretching of C=C bonds of aromatic rings, and can be associated with lignin which has many of these groups in its chemical structure.[40] In the spectra of bleached fibers and cellulose nanowhiskers,

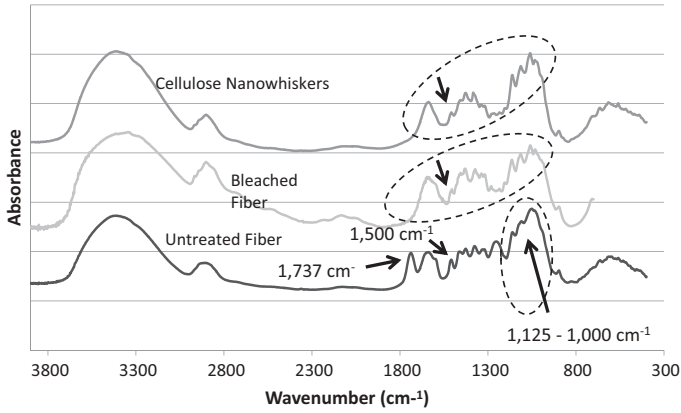

Figure 1.
FTIR spectra of the untreated fibers, bleached fibers, and cellulose nanowhiskers.

there was a significant reduction of this band that may be associated with lignin removal.

The band at 1737 cm^{-1} (highlighted in Figure 1) in the spectrum of untreated fibers is associated with the stretching of C=O groups linked to aliphatic carboxylic acid and ketone, and could be related to the hemicellulose.[41] This peak disappeared in the treated fibers and cellulose nanowhiskers, and indicating that the chemical treatments efficiently remove the hemicelluloses.

The absorption band at 1645 cm^{-1} is mainly related to the angular deformation of the water.[42] This absorption band can be observed in bleached cellulose fibers and nanowhiskers spectra, indicating that these materials become more hydrophilic when the cellulose is more exposed.

According Bahrin *et al.*,[44] the major bands associated with cellulose are between 1420 and 1430 cm^{-1}, which correspond to the structure of the amorphous/crystalline cellulose. These bands can be better observed in the bleached fibers and the cellulose nanowhiskers.

The absorption bands observed in the range of 1320–1380 cm^{-1} in all samples were attributed to the bending vibration of CO and CH groups present in the polysaccharides glycosidic rings.[45] At the same time, the bands between 1371 cm^{-1} and 1382 cm^{-1}, better visualized in the cellulose nanowhiskers, reflect the flexion of CH bond in polysaccharides.[45] The presence of absorption bands in anomeric carbon region (950–700 cm^{-1}) indicates a typical structure of cellulose.[40]

X-Ray Diffraction

Figure 2 shows the X-ray diffraction (XRD) profile of the mango starch, untreated fibers, bleached fibers, and cellulose nanowhiskers.

In the mango starch spectrum, it was possible to identify the diffraction peaks of greater intensity at angles $2\theta = 11.62°$, 15.12°, 17.14° and 23.1°. This profile corresponds to the crystallinity pattern in X-ray diffraction of type A, the same diffraction pattern is reported for corn starch.[46] The default type A which occurs in most grains is described as the organization of double helices of amylopectin macromolecules, and is the highly condensed crystalline monoclinic form.[47,48]

According to the results of XRD diffraction patterns of the samples of fibers and cellulose nanowhiskers, polymorphs of cellulose type I and type II (as described by Ford, et al.[49]) were exhibited. The diffraction peaks around $2\theta = 22$ (used to calculate the crystallinity index) become narrower and more defined after chemical treatments. This indicates the removal of amorphous material (lignin

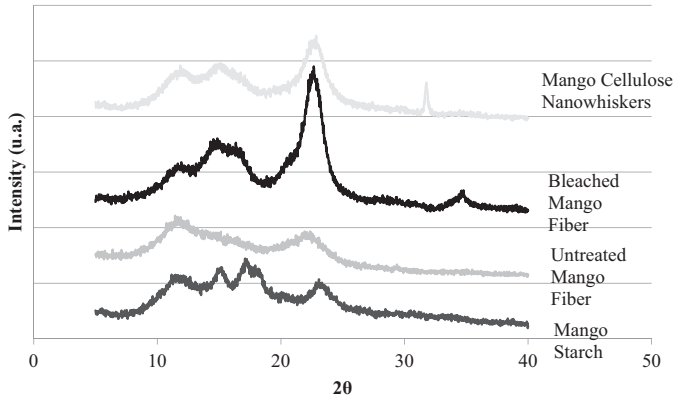

Figure 2.
Profile of the X-ray diffraction of the starch, untreated fibers, bleached fibers, and cellulose nanowhiskers obtained from mango.

Table 3.
Crystallinity index (I_{CR}) of untreated fibers, bleached fibers, and cellulose nanowhiskers.

Samples	I_{CR} (%)
Untreated Fibers	29.4
Bleached fibers	69.8
Cellulose Nanowhiskers	58.0

and hemicellulose), as already reported in previous characterizations, and consequently a considerable increase in crystallinity (Table 3).

It may be noted that there was a decrease in the crystallinity index of cellulose nanowhiskers in comparison to bleached fibers (Table 3). This result indicated that the extraction conditions used may have caused degradation of the cellulose chains,[50] and thus reduced crystallinity. The crystallinity index calculated for cellulose nanowhiskers obtained from the mango was 58%, whereas the value found for cellulose nanowhiskers obtained from the bagasse of sugar cane, coconut, rice husk, and cotton was 60%, 65. 9%, 76%, and 91%, respectively.[51–54]

Thermogravimetry

Figure 3 shows the curves of thermogravimetry (TGA and DTG) for mango starch. When starch is heat treated, it initially passes through a series of irreversible modifications with polymer structural changes and the formation of water-soluble products. The decomposition of the starch occurs, if the applied temperature exceeds 300 °C. First, structural change of the polymer occurs, generating pyrodextrins as products. At higher temperatures, the decomposition of the macromolecules leads to the formation of levoglucosanas, furfural, and finally volatile carbonaceous products of lower molecular weight.[55]

In the TGA and DTG curves, two thermal events of mass loss for mango starch can be observed. The first event corresponds to a weight loss of 11% associated with evaporation of volatiles (mainly water absorbed). The second event, given by the DTG peak with temperature of 321 °C, is related to the thermal degradation step of the starch main components (amylose and amylopectin) and minor constituents such as proteins and lipids.

The TGA and DTG curves of untreated fibers, bleached fibers, and cellulose nanowhiskers exhibited similar behavior. Two events can be identified (Figure 4): The first, for the untreated fibers, bleached fibers, and nanowhiskers at 71, 72 and 57 °C shows a loss of mass of 8, 7, and 7% respectively, which corresponds to the evaporation of volatile substances in all samples. The second thermal event refers to thermal degradation, mainly cellulose

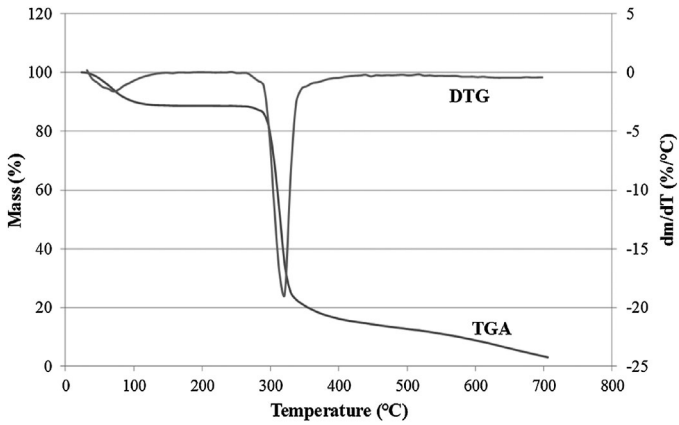

Figure 3.
TGA/DTG curves of the mango starch.

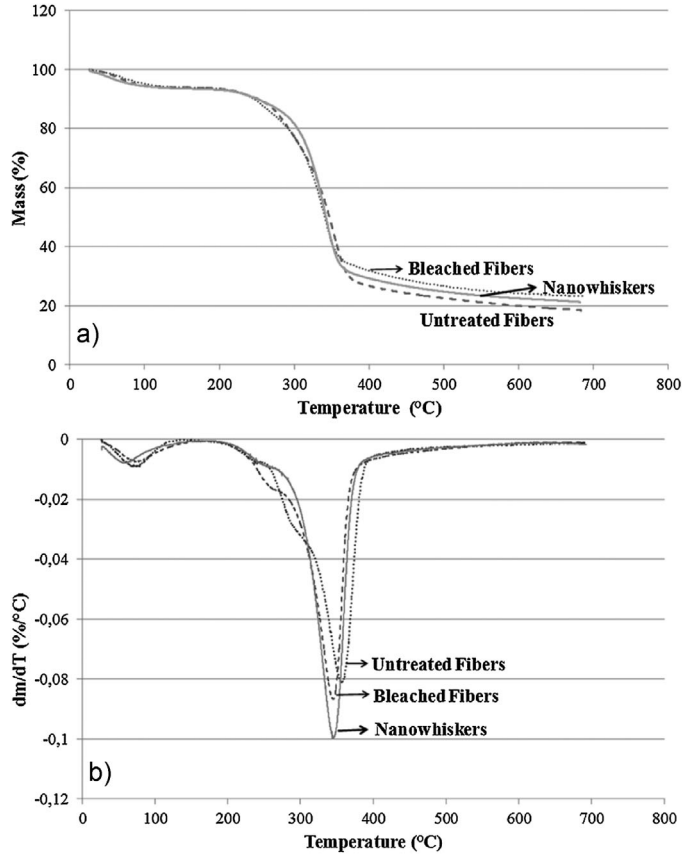

Figure 4.
TGA curves (a) and DTG (b) in untreated fibers, bleached fibers, and cellulose nanowhiskers.

(Table 2), that occurs at 356 °C for the untreated fibers, 343 °C for the bleached fibers, and 345 °C for nanowhiskers. Cellulose is the principal constituent of the fibers according to the chemical characterization (Table 2), and, according to the literature, has its degradation in the range between 250 and 345 °C.[40,56,57] This thermal event also marks the start of degradation of the remaining constituent hemicellulose and lignin present in fibers and cellulose nanowhiskers. The temperature difference between the degradation of untreated fibers, bleached fibers, and nanowhiskers can be attributed to minor surface area of untreated material, because this consists of a cluster of interconnected lignin fibers. By following the bleaching process and obtaining the nanowhiskers, the fibers are separated increasing their surface area and therefore their susceptibility to thermal degradation.

The thermal behavior analysis of the starch, bleached fibers, and cellulose nanowhiskers revealed that these materials are suitable for use in obtaining biopolymers since they have degradation temperatures above the processing temperature in the extruder to obtain TPS composites and nanocomposites.

Differential Scanning Calorimetry

The differential scanning calorimetry (DSC) was used to determine the glass transition temperature (T_g) and crystalline melting temperature (T_m) of the thermoplastic starch composites and nanocomposites. The results are presented in Table 4.

Table 4.
Glass transition temperature and crystalline melting temperature of the samples.

Samples	Glass transition temperature (T_g)			Crystalline melting temperature (T_m)	
	T_{g1} (°C)	T_{g2} (°C)	T_{g3} (°C)	Peak T_m (°C)	ΔH_m (J.g^{-1})
MS	−63	146	–	172	5.84
MS6BF	−60	95	145	168	5.22
MS1CN	−61	85	140	168	5.39
CS	−65	129	139	166	5.83
CS6BF	−63	–	140	165	5.90
CS1CN	−62	–	141	164	5.63

Mathew and Dufresne[58] reported two increases in the specific heat of plasticized starch with glycerol, related to the partial miscibility between glycerol and starch that were associated with the transition from the rubbery state of the vitreous phase rich in glycerol (low transition temperature), and the amylopectin-rich phase (transition from high temperature).

The first T_g was found for all samples ranged from −63 to −60 °C, these values can be attributed to the glass transition temperature of glycerol (plasticizer), which occurs at temperatures around −50 °C, according to Corradini *et al.*[14] The second and third T_g are related to the thermoplastic starch.

The melting temperatures (T_m) of TPS composites and nanocomposites showed the minimum value of 164 °C for sample CS1CN and maximum of 172 °C for MS (Table 4). It is observed that the initial T_m is slightly reduced with the addition of cellulose fibers and nanowhiskers.

Transmission Electron Microscopy

Figure 5 shows a TEM micrograph of a dilute suspension of cellulose nanowhiskers extracted by acid hydrolysis. Was verified the existence of cellulose nanowhiskers in a form of needles with an average diameter (D) of 28 ± 9 nm and an average length (L) of 285 ± 116 nm, resulting in an aspect ratio (L/D) of 11.

The transmission electron microscopy confirms the effectiveness of acid hydrolysis in provide the transverse cleavage of the amorphous domains of cellulose fibers, facilitating the hydrolytic cleavage of glycosidic bonds, and partially reducing the diameter of the crystalline region.[59–60]

Cellulose nanowhiskers were obtained from various sources and had an aspect ratio of 39 ± 16 for the cellulose nanowhiskers of the coconut shell[52] and 10.7 for cotton.[54] Nanowhiskers with an aspect ratio of less than 10 do not result any improvements in the mechanical properties when used as reinforcement in polymer matrices when compared to conventional micronized fibers; only nanowhiskers with an aspect ratio of greater than 50 can achieve an efficient reinforcing effect.[61] Thereby, the cellulose nanowhiskers extracted from the mango endocarp fibers have low potential as reinforcing filler in nanocomposites.

Scanning Electron Microscopy

The micrograph (Figure 6) shows mango starch granules with an oval shape and an

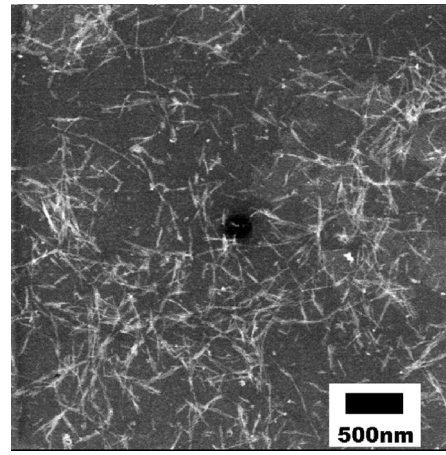

Figure 5.
TEM of the cellulose nanowhiskers extracted by acid hydrolysis of the mango endocarp fibers.

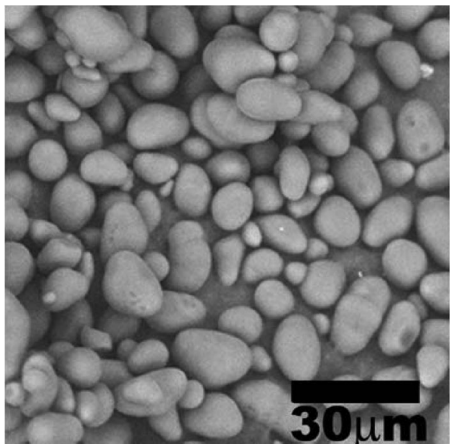

Figure 6.
SEM images of starch extracted from the mango kernels.

average diameter of 9.26 μm. The sizes of the granules are classified as small, since the mean diameter is less than 10 μm.[63] Small granules may absorb a greater amount of water compared to large ones, due to the increase of contact area.[64]

The corn starch granules are larger than those of mango starch, in the range 10 to 15 μm with round, oval and polygonal formats.[34] Oval and spherical shape require less mechanical energy during processing than polygonal shaped granules, resulting in greater water retention and ease of interaction between the OH glycerol groups.[65]

Figure 7a shows that the untreated fibers have a very packed surface due to the presence of substances that bind the fibers together: hemicelluloses and lignin. There are many impurities on the surface of untreated fiber. The subsequent bleaching treatments partially remove such material (Fig. 7b), promoting breakdown of the fibers and exposure of the pulp.

The mango TPS (Figure 8a) has compact structure, absence of cracks and bubbles, and a homogeneous appearance of starch granules (not fully plasticized) in the surface. While corn TPS (Figure 8b) does not show starch granules, that reveals the fully plasticization of the corn starch.

This difference was not expected due the similarities found between corn and mango starch in chemical and morphological analysis. But DSC results for mango and corn TPS (Table 4) showed a higher T_m for mango TPS, confirming that the processing conditions were better fitted to the corn starch than to the mango starch, as showed in the SEM images.

This difference among mango and corn TPS was confirmed by DSC results (Table 4) that shows a higher T_m for mango TPS. Thus, the processing conditions were better fitted to the corn starch than to the mango starch.

Figures 8c and 8d show the morphology of the mango and corn TPS composites with

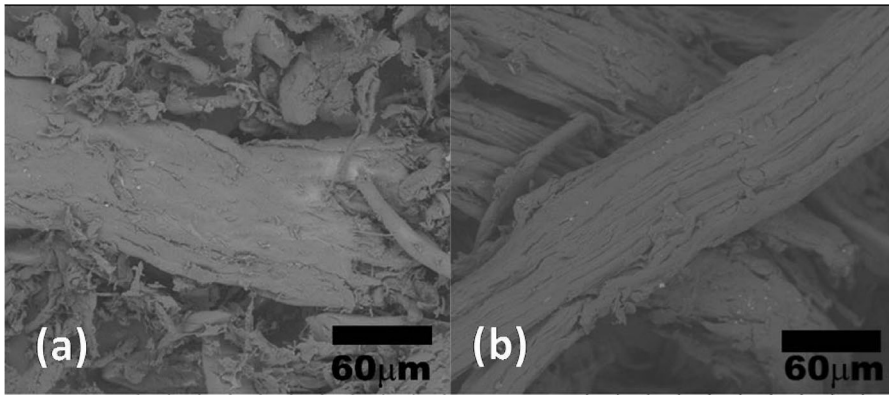

Figure 7.
SEM images of untreated fiber (a); SEM images of the bleached fiber (b).

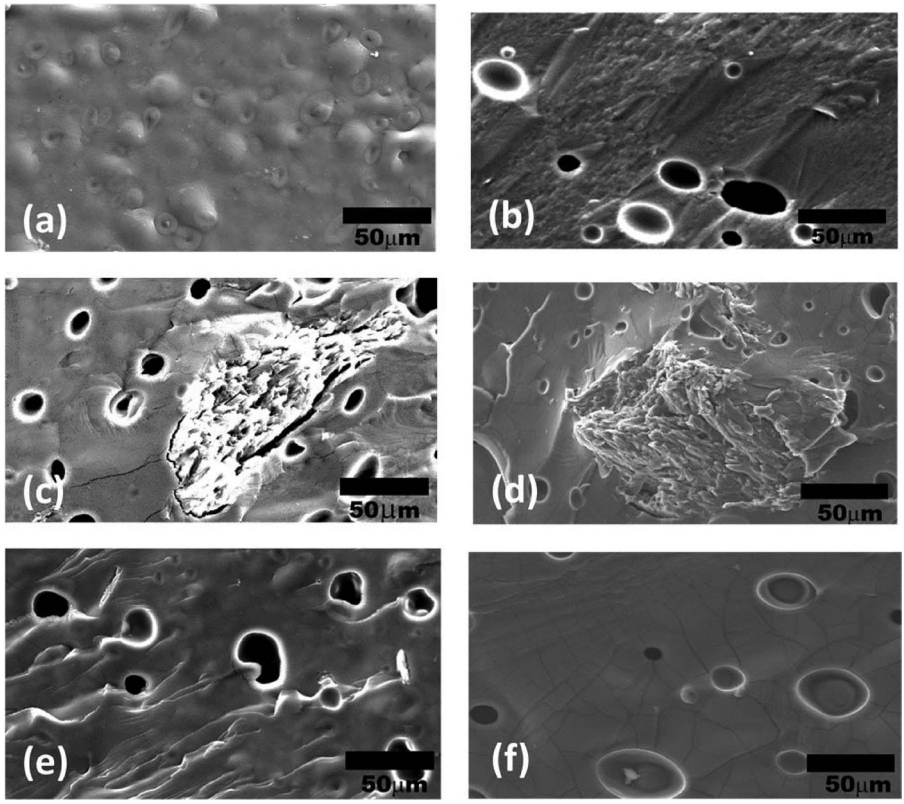

Figure 8.
SEM images of samples MS (a), CS (b) MS6BF (c) CS6BF (d) MS1CN (e) and CS1CN (f).

6% bleached fibers, MS6BF and CS6BF, respectively. There is more interfacial adhesion between fibers and matrix in the CS6BF composite than the MS6BF composite, what was revealed by the absence of voids at the interface with the matrix fibers in the CS6BF composite.

Figures 8e and 8f show the SEM images of nanocomposites of mango TPS/cellulose nanowhiskers (MS1CN) and corn TPS/cellulose nanowhiskers (CS1CN). It is observed that the SEM images of nanocomposites allowed an overview of its surface, but it has not been possible to visualize the nanostructures due to the SEM resolution. There is a porous surface in the MS1CN sample (Figure 8e), and similar results were obtained for the CS1CN sample (Figure 8f), although less intense.

The pores visualized in most samples (Figure 8) indicate that air entrapment were formed during the extrusion processing. This problem could be prevented by using molding injection to produce the samples.

Mechanical Properties

Table 5 presents the average values of maximum strength, elongation at break, and Young's modulus of TPS, TPS composites and nanocomposites produced with mango starch (MS) and corn starch (CS).

The mango TPS samples had better performance in the mechanical test than the corn TPS ones.

The Young's modulus for mango TPS, mango TPS composites and nanocomposites was higher than the same samples produced with corn starch.

The tensile strength and elongation at break for the mango TPS was greater than the mango TPS composites and nanocomposites because the porous formations

Table 5.
Data tensile strength, elongation, and Young's modulus of TPS, TPS composites and nanocomposites.

Samples	Tensile strength (MPa)	Elongation at break (%)	Young's modulus (MPa)
MS	2.77 ± 0.24	28.80 ± 2.80	46.20 ± 4.35
MS6BF	2.00 ± 0.15	16.92 ± 4.82	49.97 ± 3.62
MS1CN	2.37 ± 0.15	22.99 ± 1.70	42.80 ± 2.07
CS	2.25 ± 0.14	23.63 ± 2.12	31.83 ± 1.57
CS6BF	2.18 ± 0.13	19.84 ± 2.90	43.51 ± 2.65
CS1CN	2.43 ± 0.13	23.75 ± 1.89	35.51 ± 2.35

during processing, those porous concentrate the stress and facilitate the crack formation. For the mango TPS composites the poor interfacial adhesion of the bleached fibers and matrix also contribute to the observed results. To the corn TPS there is no difference in the values of the tensile strength and elongation break, probably related with the small variation in the porosity of the samples.

Permeability to Water Vapor

Table 6 shows the values of the thickness and the results of the permeability to water vapor (P_{WV}) of the films obtained from TPS, TPS composites and nanocomposites. It is observed that the mango TPS showed lower P_{WV}, i.e. it was less hydrophilic than the others. The MS6BF composite and the MS1CN nanocomposite showed similar results and higher than TPS, therefore more hydrophilic. This result can be explained by the poor interfacial adhesion between fiber and matrix, which reduced the efficiency of the fillers to improve the barrier properties of the polymer films.

For biopolymers produced from corn starch, the nanocomposite (CS1CN) showed higher P_{WV}, thus the composition was more hydrophilic. While the TPS (CS) and composite (CS6BF) showed lower P_{WV} values, demonstrating that the addition of bleached fibers did not reduce or even improve barrier properties.

Conclusion

The method of starch extraction from the kernels of mango pits was efficient, and the obtained starch answer the requirements of the Brazilian legislation on food production.

Chemical treatments performed on the fibers were efficient at removing the amorphous constituents (hemicellulose and lignin) and cellulose nanowhiskers from the mango endocarp were efficiently obtained.

The waste generated during processing of the mango agro-industry has potential for the production of biodegradable materials by extrusion and the performance of these materials could be improved using the injection molding.

Acknowledgements: This work was supported by the Brazilian research funding agencies CNPq, CAPES, and FINEP. The authors would like to thank EMBRAPA for supporting the laboratory infrastructure.

Table 6.
The thickness of the films and the results of the water vapor permeability of the materials obtained from the TPS composites and nanocomposites.

Material	Thickness (mm)			P_{VA} (g.mm.KPa^{-1}.h^{-1}.m^{-2})		
	TPS	6BF	1CN	TPS	6BF	1CN
Mango (MS)	0.30 ± 0.02	0.39 ± 0.02	0.33 ± 0.02	10.8 ± 0.9	12.6 ± 0.8	12.0 ± 0.8
Corn (CS)	0.34 ± 0.02	0.28 ± 0.02	0.38 ± 0.02	9.7 ± 0.7	9.4 ± 0.7	12.3 ± 0.7

[1] ABIPLAST. Associação Brasileira da Indústria do Plástico. São Paulo, 2011. http://www.abiplast.org.br. April 20, **2013**.
[2] C. T. Ferreira, J. B. F. Fonseca, C. Saron, *Polímeros* **2011**, *21*(2), 118.
[3] L. Shen, E. Worrell, M. Patel, *Biofpr, Biofuels, Bioprod. Bioref.* **2010**, *4*, 25.
[4] X. Chen, M. Khanna, *Energy Policy*. **2012**, *44*, 153.
[5] IBGE. In *Produção Agrícola Municipal*. Rio de Janeiro, **2011**.
[6] P. A. F. Vieira, Master Thesis, Bioquímica Agrícola, Universidade Federal de Viçosa, Viçosa, **2007**, 92.
[7] D. F. P. Silva, D. L. Siqueira, C. S. Pereira, L. C. C. Salomão, T. B. Struiving, *Rev. Ceres* **2009**, *56*(6), 783.
[8] J. C. Medina, E. W. Bleinroth, Z. J. Martin, D. G. Quast, T. Hashizume, N. M. S. Figueiredo, V. A. Moretti, W. L. Canto, L. C. Bicudo Neto, *Serie Frutas Tropicais*, Campinas: IMESP, **1981**, *8*, 399.
[9] A. L. da Róz, *PhD Thesis*, Ciências e Engenharia de Materiais, Instituto de Física de São Carlos e Instituto de Química de São Carlos, Universidade de São Paulo, São Paulo **2004**, 201.
[10] P. M. Forssell, J. M. Mikkilä, G. K. Moates, R. Parker, *Carbohydr. Poly*. **1998**, *34*, 275.
[11] J. Prachayawarakorn, P. Sangnitidej, P. Boonpasith, *Carbohydrate Polymers* **2010**, *81*, 425.
[12] A. Curvelo, A. J. F. Carvalho, J. A. M. Agnelli, *Carbohydr. Polym.* **2001**, *45*, 183.
[13] X. Ma, J. Yu, J. F. Kennedy, *Carbohydr. Polym.* **2005**, *62*, 19.
[14] E. Corradini, E. M. Teixeira, J. A. M. Agnelli, L. H. C. Mattoso, *Amido termoplástico*. Embrapa Instrumentação Agropecuária. São Carlos, SP, **2007**, 27.
[15] J. Prachayawarakorn, P. Ruttanabus, P. Boonsom, *J. Polym. Environ.* **2011**, *19*, 274.
[16] E. M. Teixeira, C. Lotti, A. C. Corrêa, K. B. R. Teodoro, J. M. Marconcini, L. H. C. Mattoso, *J. Appl. Polym. Sci.* **2011**, *120*, 2428.
[17] A. Campos, K. B. R. Teodoro, E. M. Teixeira, A. C. Corrêa, J. M. Marconcini, D. F. Wood, T. G. Williams, L. H. C. Mattoso, *Polym. Eng. and Sci.* **2013**, *53*, 800.
[18] M. Hietala, A. P. Mathew, K. Oksman, *Eur. Polym. J.* **2013**, *49*, 950.
[19] N. Singh, K. S. Sandhu, M. Kaur, *J. Food Eng.* **2004**, *63*(4), 441.
[20] W. J. Orts, J. Shey, S. H. Imam, G. M. Glenn, M. E. Guttman, J. F. Revol, *J. Polym. Environ.* **2005**, *13*(4), 301.
[21] IAL. INSTITUTO ADOLFO LUTZ (São Paulo,Brasil). *Métodos Físico-Químicos para análise de Alimentos: normas analíticas do Instituto Adolfo Lutz*. São Paulo; **2004**.
[22] International Organization for Standardization. Norme internationale: Riz – Détermination de la teneur em amylose. (ISO 6647). **1987**, 5.
[23] TAPPI. T 203 cm-99. Alpha-, beta- and gamma-cellulose in pulp. **2009**, 5.
[24] TAPPI. T 204 cm-97. Solvent extractives of wood and pulp. **1997**, 4.
[25] TAPPI. T 211 om-02. Ash in wood, pulp, paper and paperboard: combustion at 525 °C. **2002**, 5.
[26] TAPPI. T 222 om-02. Acid-insoluble lignin in wood and pulp. **2002**, 5.
[27] TAPPI. T 550 om-03. Determination of equilibrium moisture in pulp, paper and paperboard for chemical analysis. **2008**, 8.
[28] L. E. Wise, M. Murphy, A. A. D'Addiecs, *Pap. Trade J.* **1946**, *122*(2), 11.
[29] M. L. M. Mendes, *PhD Thesis*, Ciência e Tecnologia de Alimentos, Centro de Tecnologia, Universidade Federal da Paraíba, João Pessoa, Paraíba, **2011**, 132.
[30] A. Buléon, P. Colonna, V. Planchot, S. Ball, *Int. J. Biol. Macromol.* **1998**, *23*, 85.
[31] C. Medina, A. Paredes, M. E. Rodríguez, M. Moreno, D. Belén-Camacho, D. García, C. Ojeda, *Bioagro* **2010**, *22*, 67.
[32] S. N. Moorthy, *Tuber Crop Starches*. Thiruvananthapuram: Central Tuber Crops Research Institute, 2ed. **2001**, 52.
[33] O. Lopez, M. A. Garcia, M. A. Villar, A. Gentili, M. S. Rodriguez, L. Albertengo, *Food Sci. Technol.* **2014**, *57*, 106.
[34] V. E. Solis, *PhD Thesis*, Dessarollo de Productos Bióticos, Centro de Dessarollo de Productos Bióticos, Instituto Politécnico Nacional, Yautepec, Morelos. **2008**, 100.
[35] BRASIL. Decreto n° 12.486, de 20 de outubro de 1978. Diário Oficial do Estado de São Paulo, São Paulo, **1978**, 20.
[36] J. C. Agustiano-Osornio, R. A. González-Soto, E. Flores-Huicochea, N. Manrique-Quevedo, L. Sanchez-Hernandez, L. A. Bello-Pérez, *J. Sci. Food Agric.* **2005**, *85*, 2105.
[37] L. S. Guinesi, A. L. Da Róz, L. H. C. Mattoso, E. M. Teixeira, A. A. S. Curvelo, *Thermochim. Acta* **2006**, *447*, 190.
[38] R. M. Rowell, J. S. Han, J. S. Rowell, *Embrapa Instrumentação Agropecuária*, Brasil, **2000**, 115.
[39] H. Yang, R. Yan, H. Chen, D. H. Lee, C. Zheng, *Biotechnol. Biofuels* **2007**, *86*, 1781.
[40] B. Xiao, X. F. Sun, R. C. Sun, *Polymer Degradation and Stability* **2001**, *74*, 307.
[41] N. Sgriccia, M. C. Hawley, M. Misra, *Composites, Part A* **2008**, *39*, 1632.
[42] E. M. Teixeira, *PhD Thesis*, Físico-química, Instituto de Química de São Carlos, Universidade de São Paulo, São Paulo. **2007**, 201.
[43] H. P. A. Khalil, H. Ismail, H. D. Rozman, M. N. Ahmad, *European Polymer Journal* **2001**, *37*, 1037.
[44] E. K. Bahrin, A. S. Baharuddin, M. F. Ibrahim, M. N. Abdul Razak, A. Sulaiman, S. Abd-Aziz, M. A. Hassan, Y. Shirai, H. Nishida, *BioResources* **2012**, *7*, 1784.
[45] M. Troedec, D. Sedan, C. Peyratout, J. Bonnet, A. Smith, R. Guinebretiere, V. Gloaguen, P. Krausz, *Composites, Part A* **2008**, *39*, 514.
[46] T. Y. Bogracheva, Y. L. Wang, T. L. Wang, C. L. Hedley, *Biopolymers* **2002**, *64*, 268.
[47] C. G. Oates, *Trends Food Sci. Technol.* **1997**, *8*, 375.

[48] A. C. Eliasson, *Starch in food – Structure, function and applications*, CRC, New York **2004**.
[49] E. N. J. Ford, S. K. Mendon, S. F. Thames, J. W. Rawlins, *J. Eng. Fibers Fabr.* **2010**, *5*, 10.
[50] A. C. Corrêa, E. M. Teixeira, J. M. Marconcini, L. A. Pessan, L. H. C. Mattoso, *Anais do 10° Congresso Brasileiro de Polímeros* Foz do Iguaçu, PR, **2009**.
[51] J. Li, X. Wei, Q. Wang, J. Chen, G. Chang, L. Kong, J. Su, Y. Liu, *Carbohydr. Polym.* **2012**, *90*, 1609.
[52] M. F. Rosa, E. S. Medeiros, J. A. Malmonge, K. S. Gregorski, D. F. Wood, L. H. C. Mattoso, G. Glenn, W. J. Orts, S. H. Imam, *Carbohydr. Polym.* **2010**, *81*, 83.
[53] L. Ludueña, D. Fasce, V. A. Alvarez, P. M. Stefani, *BioResources* **2011**, *6*, 1440.
[54] M. A. Martins, E. M. Teixeira, A. C. Corrêa, M. Ferreira, L. H. C. Mattoso, *J. Mater. Sci.* **2011**, *46*, 7858.
[55] P. Aggarwal, D. Dollimore, *Thermochim. Acta* **1998**, *447*, 17.
[56] J. I. Morán, V. A. Alvarez, V. P. Cyras, A. Vázquez, *Cellulose* **2008**, *15*, 149.
[57] S. M. L. Rosa, N. Rehman, M. I. G. Miranda, S. M. B. Nachtigall, C. I. D. Bica, *Carbohydr. Polym.* **2012**, *87*, 1131.
[58] A. P. Mathew, A. Dufresne, *Biomacromolecules* **2002**, *3*, 1101.
[59] M. A. S. Azizi Samir, F. Alloin, A. Dufresne, *Biomacromolecules* **2005**, *6*, 612.
[60] F. Fahma, S. Iwamoto, N. Hori, T. Iwata, A. Takemura, *Cellulose* **2010**, *17*, 977.
[61] S. J. Eichhorn, A. Dufresne, M. Aranguren, N. E. Marcovich, J. R. Capadona, S. J. Rowan, C. Weder, W. Thielemans, M. Roman, S. Renneckar, W. Gindl, S. Veigel, J. Keckes, H. Yano, K. Abe, M. Nogi, A. N. Nakagaito, A. Mangalam, J. Simonsen, A. S. Benight, A. Bismarck, L. A. Berglund, T. Peijs, *J. Mater. Sci.* **2010**, *45*, 1.
[62] F. Dalmas, J. Y. Cavaillé, C. Gauthier, L. Chazeau, R. Dendievel, *Compos. Sci. Technol.* **2007**, *67*, 829.
[63] P. G. Yonemoto, M. A. Calori-Domingues, C. M. L. Franco, *Ciência e Tecnologia de Alimentos* **2007**, *27*, 761.
[64] O. Paredes-López, M. L. Schevenin, D. Hernandéz-Lopéz, A. Cárabez-Trejo, *Starch/Stärke* **1989**, *41*, 205.
[65] T. Galicia-García, F. Martínez-Bustos, O. A. Jiménez-Arévalo, D. Arencón, J. Gámez-Pérez, A. B. Martínez, *J. Appl. Polym. Sci.* **2012**, *126*, 327.

